Investigating the pairing state of cuprate superconductors via quasiparticle tunneling and spin injection[1]

N.-C. Yeh[a,*], C.-T. Chen[a], C.-C. Fu[a], P. Seneor[a], Z. Huang[a], C. U. Jung[b], J. Y. Kim[b], Min-Seok Park[b], Heon-Jung Kim[b], S.-I. Lee[b], K. Yoshida[c], S. Tajima[c], G. Hammerl[d], and J. Mannhart[d]

[a] *Department of Physics, California Institute of Technology, Pasadena, CA 91125, USA*
[b] *National Creative Research Initiative Center for Superconductivity, Pohang University of Science and Technology, Pohang 790-784, Korea*
[c] *Superconductivity Research Laboratory, International Superconductivity Technology Center, Tokyo, Japan*
[d] *Center for Electronic Correlations & Magnetism, Institute of Physics, Augsburg University, Augsburg, Germany*

Received 24, June 2001

Abstract

Scanning tunneling spectroscopic studies of cuprate superconductors revealed that the most eminent phenomena of hole-doped (p-type) cuprates, including the predominant $d_{x^2-y^2}$ pairing symmetry, spin fluctuations and pseudogap, are absent in the infinite-layer electron-doped (n-type) cuprates $Sr_{1-x}La_xCuO_2$. The optimally doped $Sr_{0.9}La_{0.1}CuO_2$ exhibits *s*-wave pairing symmetry, with a superconducting transition temperature $T_c = 43.0$ K, a large energy gap $\Delta = 13.0 \pm 1.0$ meV, and no pseudogap in the normal state. The response of $Sr_{0.9}La_{0.1}CuO_2$ to quantum impurities is also conventional, being less sensitive to non-magnetic impurities than to magnetic impurities, in sharp contrast to the strong effects induced by static non-magnetic impurities in the p-type cuprates. The dynamic injection of spin-polarized quasiparticles is found to incur significant suppression of superconductivity into the p-type cuprates, probably due to the strong influence on the spin fluctuations.

PACS: 74.50.+r; 74.72.-h; 74.40.+k; 74.80.Dm
Keywords: Cuprate superconductors; Tunneling spectroscopy; Pairing symmetry; Nonequilibrium superconductivity

1. Introduction

The $d_{x^2-y^2}$-wave pairing symmetry [1,2], spin fluctuations [3], and pseudogap phenomena in the under- and optimally hole-doped (p-type) cuprates [3-5] have been regarded as highly relevant to the pairing mechanism of high-temperature superconductivity. On the other hand, the exact pairing symmetry and the existence of pseudogap phenomena in the electron-doped (n-type) cuprates $Ln_{2-x}Ce_xCuO_{4-\delta}$ (Ln = Nd, Pr, Sm) still remain controversial [6,7]. A number of the theories have centered on the viewpoint that the pseudogap is a precursor for superconductivity [3-5]. Some models such as the resonant-valence-bond (RVB) [8] and *SU(2)* slave-boson scenarios [9,10] have suggested that the pseudogap is associated with the formation of pairing in the spin channel at $T^* >> T_c$, and that superconductivity occurs at T_c due to the Bose-Einstein condensation of holons. Others suggested that charged stripes with preformed Cooper pairs may exist in the pseudogap regime (i.e., at $T_c < T < T^*$), and Josephson coupling among stripes is established at $T < T_c$ [11,12]. The non-Fermi liquid (NFL) behavior in the normal-state of optimally and under-doped regimes and the Fermi liquid (FL) behavior in the overdoped regime

* Corresponding author.
E-mail address: ncyeh@caltech.edu

[1] The work at Caltech is supported by NSF DMR-0103045, at Pohang University by the Ministry of Science and Technology of Korea, University of Augsburg by BMBF #13N6918/1, and at SRL/ISTEC by New Energy Industrial Technology Development Organization.

of the p-type cuprates has also motivated a conjecture of a quantum critical point (QCP) in the ground state of the cuprates [13]. This view differs fundamentally from the preformed pair scenarios. Other viewpoints include the consideration of competing orders in the ground state of the doped Mott antiferromagnet by studying the effects of increasing doping levels and varying strengths of the Coulomb interaction [14], which could also lead to the occurrence of a QCP.

In this work, we report experimental studies of the pairing state of both p-type and n-type cuprates. Our findings in the infinite-layer n-type cuprates counter several widely accepted viewpoints in the p-type cuprates, and we suggest that the pair formation does not depend on the pairing symmetry, the existence of a pseudogap, or the presence of spin fluctuations.

2. Doping-dependent pairing state of the p-type cuprates

A rigorous proof for the existence of a QCP must identify the associated broken symmetry. Moreover, if the existence of a QCP were relevant to the pairing mechanism, a universal broken symmetry should be expected in all cuprate superconductors. We have recently investigated the quasiparticle tunneling spectra of the $YBa_2Cu_3O_{7-\delta}$ system (YBCO) in the optimally and under-doped regime and $(Y_{0.7}Ca_{0.3})Ba_2Cu_3O_{7-\delta}$ in the overdoped regime [15,16], and found that the pairing symmetry evolves from the predominantly $d_{x^2-y^2}$-wave (>95%) pairing in the under- and optimally doped regime to mixed pairing symmetries of $(d_{x^2-y^2}+s)$ with the *s*-component exceeding *30%*, as exemplified by the c-axis quasiparticle tunneling spectra in Figure 1. Although our data indicated a significant increase in the *s*-wave component with the increasing doping level in YBCO, we could not conclude the existence of a QCP associated with a broken C_{4v} symmetry, because YBCO is known to exhibit slight orthorhombicity (*~2%*) in the under- and optimally doped regime. For comparison, in the tetragonal system of Bi-2212 ($Bi_2Sr_2CaCu_2O_x$), the pairing symmetry has always been consistent with pure $d_{x^2-y^2}$ for all doping levels [17-19], thus no obvious broken symmetry at a critical doping level. Concerning the possibility of broken time-reversal ($\boldsymbol{T}$) symmetry, the scanning tunneling spectral characteristics of YBCO [15,16] and Bi-2212 [17-20] systems have revealed no evidence for complex pairing symmetries such as $(d_{x^2-y^2}+is)$ or $(d_{x^2-y^2}+id_{xy})$. Although tunneling spectra cannot detect certain types of broken $\boldsymbol{T}$-symmetry such as the staggered flux state [21,22] or the circulating current phase [13], there has not been conclusive evidence for a QCP with a universal broken symmetry. Recently, an *SU(2)* slave-boson approach to the *t-J* Hamiltonian [23] has found that under the constraint of no double occupancy, the inclusion of spinon and holon interactions and the assumption of $d_{x^2-y^2}$-wave spinon pairing at T^* leads to an *s*-wave symmetry for the holon-pair condensation at $T_c < T^*$ in the under- and optimally doped regime, and T_c merges with T^* in the overdoped regime. Thus, the pairing symmetry could crossover from $d_{x^2-y^2}$ to $(d_{x^2-y^2}+s)$ in the overdoped regime without encountering a QCP.

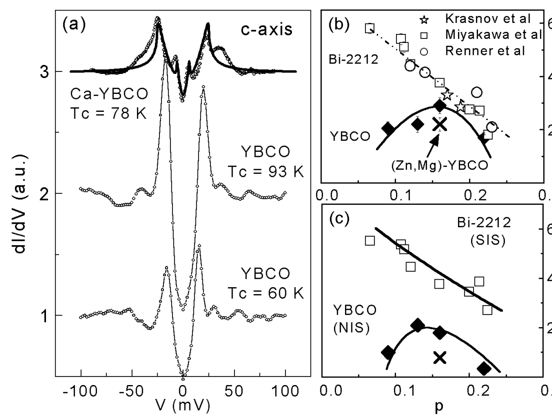

Fig. 1. (a) Representative c-axis tunneling spectra of YBCO with different doping levels, showing $d_{x^2-y^2}$ pairing symmetry for the underdoped and optimally doped YBCO, and $(d_{x^2-y^2}+s)$ symmetry in the overdoped YBCO, with a significantly large *s*-wave component. (b) The doping dependence of the pairing potential Δ_d and (c) the spin resonant energy $\boldsymbol{\Omega}_{res}$ associated with the satellite features [15,16], together with the results from Bi-2212 [17-19].

A natural consequence of the $d_{x^2-y^2}$ or $(d_{x^2-y^2}+s)$ pairing symmetry is the gapless nature of the pairing potential and the presence of nodal quasiparticles. Hence, quantum impurities that substitute the Cu^{2+}-ions in the CuO_2 planes are expected to incur strong effects on superconductivity [24-26] due to interactions with the nodal quasiparticles. Such effects are in contrast to the weak response of conventional *s*-wave superconductors to non-magnetic impurities [27]. In addition to the strong potential scattering, Kondo effects [28,29] are expected due to the induced magnetic moments associated with the non-magnetic impurities (such as Zn^{2+}, Mg^{2+}, Al^{3+} and Li^{+}) [30-37]. Our studies of an optimally oxygen-doped YBCO single crystal with a small concentration of Zn and Mg impurities have also revealed strong local effects on the quasiparticle spectra [15,16], as exemplified in Fig. 2.

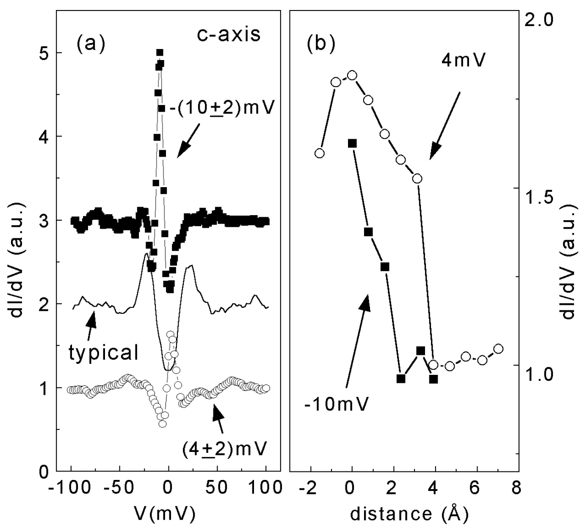

Fig. 2. (a) Nano-scale spatially varying c-axis tunneling spectra near the Zn and Mg impurities of a (Zn,Mg)-doped YBCO single crystal at T = 4.2 K. Two types of resonant scattering energies are found at (−10±2) meV and (4±2) meV, which correspond to two different substitutions of Zn and Mg in the CuO_2 planes. The typical c-axis tunneling spectrum is recovered at ~ 3 nm away from an impurity. (b) The spatial dependence of the impurity scattering peak intensity, showing rapid decrease within one Fermi wavelength (~ 0.3 nm).

In the context of pseudogap, our low-temperature tunneling data in the YBCO system differed from the finding in Bi-2212 [15,16]. In particular, the doping dependence of the gap values in YBCO appears to be correlated with T_c [15,16], in contrast to the averaged gap values determined from the Bi-2212 system that increase with decreasing doping level [17-19]. Besides the difference in the doping dependence of the gap values, no direct evidence for a pseudogap could be identified in our tunneling spectra on YBCO [15,16]. Furthermore, the spectra exhibited long-range spatial homogeneity [15,16], in sharp contrast to the nano-scale large variations in the gap value of Bi-2212 [38]. The different pseudogap behavior in two families of p-type cuprates (i.e. YBCO and Bi-2212) suggests that the pseudogap need not be a precursor of cuprate superconductivity.

3. Effects of spin-polarized quasiparticles on the superconducting state of p-type cuprates

Our studies of the quasiparticle tunneling spectra have suggested the relevance of spin fluctuations to the properties of p-type cuprates and the strong effects of static quantum impurities on the collective spin excitations [15,16]. A natural extension of the research is to investigate how dynamic injection of spin-polarized quasiparticles may affect the cuprates.

There are two primary effects associated with the injection of spin-polarized quasiparticles on a superconductor. One is the exchange interaction and broken ***T***-symmetry due to the excess magnetic moments. The other is the non-equilibrium distribution of quasiparticles and momentum shift due to the injected current. To distinguish the difference between the spin and charge relaxation processes, we compare the characteristics of cuprate superconductors under either simple or spin-polarized quasiparticle injection. It has been demonstrated that electrical currents can become spin polarized after passing through a ferromagnetic metal [39]. Based on this approach, we studied thin-film heterostructures of perovskite ferromagnet-insulator-superconductor (F-I-S) and non-magnetic metal-insulator-superconductor (N-I-S). Using pulsed current techniques to prevent artifacts from Joule heating in the critical current measurements [40,41], we have demonstrated strong suppression in the critical current density J_c of the superconductor with injection of spin-polarized currents, and much weaker suppression of J_c under similar injection current density in the N-I-S control samples. We have also performed scanning tunneling spectroscopic studies and found strong modifications in the quasiparticle density of states only under spin injection [42]. However, many important issues, particularly the microscopic interaction of spin-polarized quasiparticles with the cuprates, remain to be resolved.

The constituent layers of our F-I-S and N-I-S heterostructures consisted of either $La_{0.7}Ca_{0.3}MnO_3$ or $La_{0.7}Sr_{0.3}MnO_3$ for the ferromagnet, $SrTiO_3$ for the insulator, $YBa_2Cu_3O_{7-\delta}$ for the superconductor, and $LaNiO_3$ for the non-magnetic metal, all deposited on the $LaAlO_3$ substrate. Details of the fabrication and characterization of the thin-film heterostructures are described elsewhere [40,41]. To quantify the effects of quasiparticle injection, we compare the critical current density J_c^0 of the cuprate superconductor in the absence of quasiparticle injection with the critical current J_c

under finite injection. Here J_c is determined by the temperature (T), the injection current density (J_{inj}), and the characteristic sample dimension (d) along the direction of quasiparticle injection. We note that the spin-polarized quasiparticles generally have much longer lifetime than simple quasiparticles because of the low probabilities of being recombined into Cooper pairs. For conventional superconductors, the standard microscopic mechanisms for spin relaxation involve spin-orbit interactions and magnetic impurity scattering [43]. For p-type cuprate superconductors, interactions with the collective spin excitations can be expected.

We define the "efficiency" (η) of suppressing superconductivity due to an injection current density J_{inj} as $\eta(T,J_{inj}) \equiv \Delta J_c(T,J_{inj})/J_{inj} \equiv [J_c^0(T)-J_c(T,J_{inj})]/J_{inj}$. For a constant J_{inj}, the corresponding efficiency in F-I-S, η_s, and that in N-I-S, η_n, is illustrated in Figures 3(a) and 3(b). We find that η_s is generally larger than η_n. In addition, η_n increases with increasing J_{inj} for all T, and so does η_s at high temperatures. However, anomalous decrease in η_s with increasing J_{inj} is found at low temperatures. This seemingly surprising behavior is in fact the result of non-equilibrium distributions of Fermions, as elaborated below.

We consider the quasiparticle energy E_k under a finite injection current density J_{inj}, where $\boldsymbol{k}$ denotes the quasiparticle momentum. The quasiparticle energy in thermodynamic equilibrium is given by $E_k^0 = (\Delta_k^2 + \xi_k^2)^{1/2}$, where ξ_k ($= \varepsilon_k - \varepsilon_F$) is the single particle energy relative to the Fermi level ε_F [44]. A finite rate of quasiparticle injection can lead to modification to the quasiparticle energy and the effective temperature, therefore redistribution of quasiparticles. In the case of simple quasiparticle injection, a finite superfluid velocity $v_s = J_{inj}/(n_s e)$ can result in changes in the quasiparticle energy E_{kn} and distribution function f_{kn}:

$$E_{kn} = E_k^0 + h\boldsymbol{k}_F \bullet \boldsymbol{v}_s/(2\pi m^*) \equiv E_k^0 + \delta E_J,$$
$$f_{kn} = 1/\{1+\exp[E_{kn}/(k_BT)]\}, \qquad (1)$$

where $\boldsymbol{k}_F$ is the quasiparticle momentum at the Fermi level, and T_n* is effective temperature under simple quasiparticle injection. Using the pairing potential Δ_k consistent with the $d_{x^2-y^2}$-wave pairing in optimally doped YBCO, and the single particle energies ξ_k consistent with the tight-binding band structure calculations [45], we find that $E_k^0 >> |h\boldsymbol{k}_F \bullet \boldsymbol{v}_s/(2\pi m^*)|$ is generally satisfied in our experiments for typical injection currents. Thus, $f_{kn} \sim 0$.

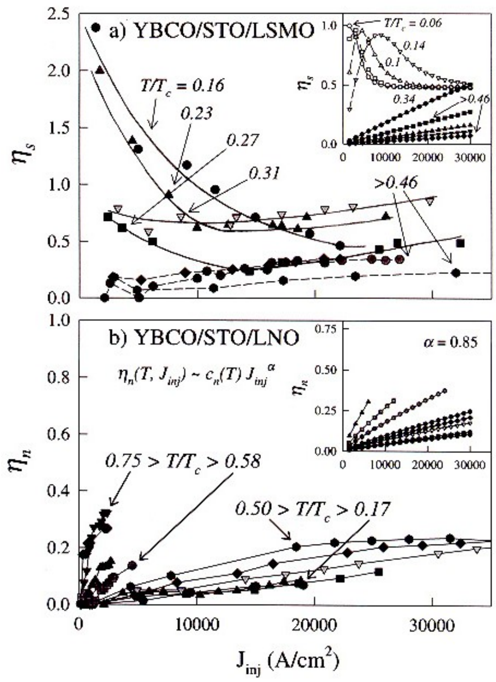

Fig. 3. (a) The efficiency (η_s) vs. injected current density (J_{inj}) of an F-I-S sample at different reduced temperatures (T/T_c). We note the rapid drop in η_s with J_{inj} only at low T and the monotonic increase of η_s with J_{inj} at high T. The inset illustrates the simulated results using Eqs. (1)-(3). (b) The efficiency (η_n) vs. J_{inj} of an N-I-S sample at different (T/T_c) values, which is proportional to J_{inj}^{α} with $\alpha \approx 0.85$.

In the case of spin-polarized quasiparticles, the long quasiparticle lifetime will lead to a chemical potential shift μ* for the quasiparticles. Thus, the quasiparticle energy E_{ks} and the distribution function f_{ks} become:

$$E_{ks}(T,J_{inj}) = [(\xi_k-\mu^*)^2+\Delta_k^2]^{1/2} + \delta E_J,$$
$$f_{ks}(T,J_{inj}) = 1/\{1+\exp[E_{ks}/(k_BT)]\}. \qquad (2)$$

Here μ* is determined by averaged spin polarization in the superconductor, $\boldsymbol{P} = \tanh(c_1J_{inj}/k_BT)$, so that $\mu^*(T,J_{inj}) = \mu_0^*\tanh(c_1J_{inj}/k_BT)$, where μ_0* and $c_1(T)$ are positive values to be determined empirically. The suppression of the critical current density ΔJ_c is proportional to the excess magnetic moments $\langle m_s\rangle$ adjusted by the available quasiparticle states, and $\langle m_s\rangle \sim J_{inj}\tanh(c_1J_{inj}/k_BT)$ takes the form of the Brillouin function for a spin-1/2 system. Thus, we express η_s and η_n as follows:

$$\eta_s \equiv \Delta J_c/J_{inj} \sim N_0^{-1}\Sigma_k(1-2f_{ks})\tanh(c_1J_{inj}/k_BT),$$
$$\eta_n \sim N_0^{-1}\Sigma_k(1-2f_{kn})\, c_n(T)J_{inj}^{\alpha} \approx c_n(T)J_{inj}^{\alpha}, \qquad (3)$$

where N_0 denotes the total number of states, $c_n(T)$ is a monotonic function of T, comparable to the normal fluid fraction of the superconductor, and $\alpha \approx 0.85$ is empirically determined. The quantity $(1-2f_{ks})$ accounts for the quasiparticle redistribution under spin injection.

Following the analysis outlined in Eqs. (1)--(3), we obtain simulated results in the insets of Figures 3(a) and 3(b). To achieve quantitative agreement with the experimental data, we find that a large chemical potential shift μ_0^* (~ 700 K) must be imposed. These strong non-equilibrium effects due to spin-polarized quasiparticles are suggestive of their unusual interactions with the cuprates, such as the suppression of collective spin excitations. These effects differ from the typical spin relaxation process in conventional superconductors via the spin-orbit interaction [46].

4. The n-type infinite-layer system: conventional superconductivity in unconventional cuprates

The infinite-layer system $Sr_{1-x}Ln_xCuO_2$ (Ln = La, Gd, Sm) has the simplest structure among all cuprate superconductors, and the optimal electron doping occurs at x = 0.1 according to the band structure calculations [47]. The $Sr_{1-x}Ln_xCuO_2$ system differs from other cuprates in that there is no extra charge block between consecutive CuO_2 planes, and the c-axis lattice constant (c_0 = 0.347 nm) is shorter than the in-plane lattice constant (a_0 = 0.390 nm). Studies of their fundamental physical properties have been limited [48-50] due to the difficulties in achieving single phase and 100% superconducting volume. Recent improvement of synthesis techniques has resulted in single-phased samples of optimally doped $Sr_{0.9}La_{0.1}CuO_2$ with T_c = 43.0 K and 100% superconducting volume [51], thus enabling our studies of the quasiparticle spectra.

For over 1000 tunneling spectra on more than 100 randomly oriented grains of a $Sr_{0.9}La_{0.1}CuO_2$ sample, long-range spatial homogeneity and little variation in the superconducting gap value from one grain to another was found. The spectral characteristics were consistently with the isotropic *s*-wave pairing symmetry and a superconducting gap Δ = 13.0 ±1.0 meV, as exemplified in the main panel of Figure 4. The unusually large ratio of $(2\Delta/k_BT_c) \approx 7.0$ relative to the BCS value 3.5 is suggestive of strong coupling effects. In addition, the "satellite features" associated with damping of quasiparticles by the spin fluctuations in p-type cuprate superconductors [15-20], as exemplified in Figure 1, were absent in $Sr_{0.9}La_{0.1}CuO_2$. These results suggest that $d_{x^2-y^2}$-wave pairing and spin fluctuations are not essential for pairing in cuprates.

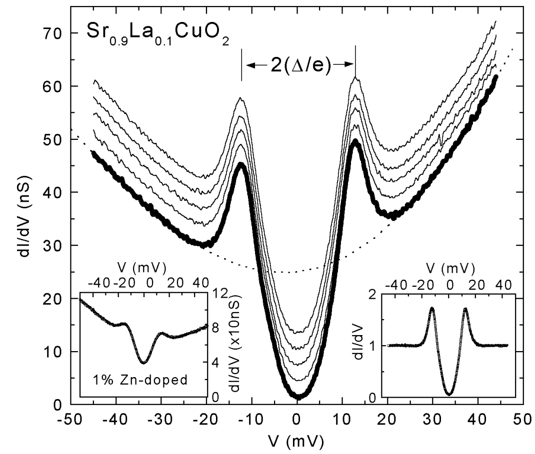

Fig. 4. Representative quasiparticle tunneling spectra of $Sr_{0.9}La_{0.1}CuO_2$, showing long-range spatial homogeneity and characteristics consistent with isotropic s-wave pairing symmetry and a large gap Δ = 13.0±1.0 meV. The inset shows a tunneling spectrum of $Sr_{0.9}La_{0.1}(Cu_{0.99}Zn_{0.01})O_2$, with a comparable Δ and the same T_c.

We have also investigated the spectral characteristics of the n-type infinite-layer system with quantum impurities. For $Sr_{0.9}La_{0.1}(Cu_{0.99}Zn_{0.01})O_2$ with non-magnetic Zn-impurities, we found similar long-range spatial homogeneity and comparable gap value, although the spectral peak height was reduced and excess density of states between the peaks was observed due to Zn-induced disorder, as exemplified in the inset of Figure 4. The spatial homogeneity was in sharp contrast to the nano-scale spatial variations in the quasiparticle spectra of Zn-doped p-type cuprates [15-20]. On the other hand, significant electron-hole spectral asymmetry was observed in the Ni-doped sample $Sr_{0.9}La_{0.1}(Cu_{0.99}Ni_{0.01})O_2$, while the gap value remained invariant, as shown in Figure 5. The spectral asymmetry represented the different phase shifts in the electron-like and hole-like quasiparticle states as the result of broken time-reversal symmetry induced by the magnetic impurities. The asymmetric phase shifts gave rise to a reduced superconducting phase coherence and thus suppression in T_c. The spectral difference for the curves in Figure 5 is illustrated in the inset, showing spectral peaks at $\Omega_{\pm}$. Similar finding of the electron-hole spectral asymmetry associated with localized magnetic impurities has also been reported in a conventional superconductor [27].

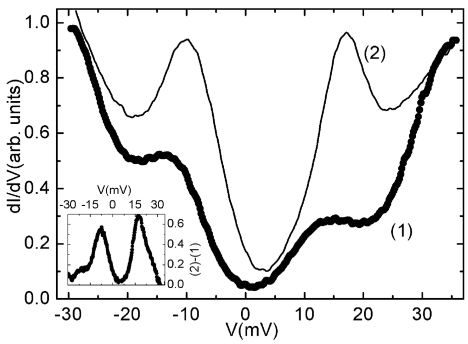

Fig. 5. Representative quasiparticle tunneling spectra of $Sr_{0.9}La_{0.1}(Cu_{0.99}Ni_{0.01})O_2$, with the majority spectra showing large electron-hole asymmetry (solid symbols) and minority spectra with electron-hole symmetry (thin solid curve). The spectral difference illustrated in the inset is due to impurity-induced resonant energies at $\Omega_{\pm}$.

5. Conclusion

We have investigated the pairing state of cuprate superconductors by means of scanning tunneling spectroscopy and spin injection. For the p-type cuprates, the pairing symmetry is primarily $d_{x^2-y^2}$ in the underdoped and optimally doped regimes and ($d_{x^2-y^2}$ $+s$) in the overdoped regime of YBCO. In addition, spin fluctuations appear to be significant and coupled strongly to the low-energy excitations of the pairing state, and the injection of spin-polarized quasiparticles results in strong suppression of spin fluctuations and superconductivity. In contrast, studies of the infinite-layer cuprate $Sr_{0.9}La_{0.1}CuO_2$ reveal *s*-wave pairing symmetry and a large gap of 13.0 ± 1.0 meV, with no evidence for either spin fluctuations or pseudogap. We therefore suggest that the $d_{x^2-y^2}$ pairing symmetry, spin fluctuations, and pseudogap need not be essential to the pairing mechanism of cuprate superconductivity.

References

[1] C. C. Tsuei, and J. R. Kirtley, *Rev. Mod. Phys.* **72,** 969-1016 (2000); and references therein.
[2] D. J. Van Harlingen, *Rev. Mod. Phys.* **67,** 515 (1995).
[3] J. Orenstein, and A. J. Millis, *Science* **288**, 468 (2000); and references therein.
[4] S. Sachdev, *Science* **288**, 475 (2000).
[5] T. Timusk and B. Statt, *Rep. Prog. Phys.* **62**, 61 (1999); and references therein.
[6] L. Alff *et al.*, *Phys. Rev. Lett.* **83**, 2644 (1999).
[7] C. C. Tsuei, and J. R. Kirtley, *Phys. Rev. Lett.* **85,** 182-185 (2000).
[8] P. W. Anderson, *Science* **235**, 1196 (1987).
[9] P. A. Lee & X. G. Wen, *Phys. Rev. Lett.* **78**, 4111 (1997).
[10] G. Kotliar, *Phys. Rev. B* **37**, 3664 (1988).
[11] V. J. Emery *et al.*, *Phys. Rev. B* **56**, 6120 (1997).
[12] G. Siebold *et al.*, *Phys. Rev. B* **58**, 13506 (1998).
[13] C. M. Varma, *Phys. Rev. B* **55**, 14554 (1997).
[14] M. Vojta *et al.*, *Phys. Rev. B* (2000).
[15] N.-C. Yeh *et al.*, *Phys. Rev. Lett.* (2001), in press.
[16] N.-C. Yeh *et al.*, *Physica C* (2001), in press.
[17] N. Miyakawa, *Phys. Rev. Lett.* **83**, 1018 (1999).
[18] Ch. Renner *et al.*, *Phys. Rev. Lett.* **80**, 149 (1998).
[19] V. M. Krosnov *et al.*, *Phys. Rev. Lett.* **84**, 5860 (2000).
[20] S. H. Pan *et al.*, *Nature* **403**, 746 (2000).
[21] I. K. Affleck and J. B. Marston, *Phys. Rev. B* **37**, 3774 (1988).
[22] S. Chakravarty and H.-Y. Kee, *Phys. Rev. B* **61**, 14821 (2000).
[23] S. S. Lee & S.-H. S. Salk, *Phys. Rev. B* (2001), in press.
[24] A. V. Balatsky *et al.*, *Phys. Rev. B* **51**, 15547 (1995).
[25] M. I., Salkola *et al.*, *Phys. Rev. Lett.* **77**, 1841 (1996).
[26] M. E. Flatte, *Phys. Rev. B* **61**, 14920 (2000).
[27] A. Yazdani *et al.*, *Science* **275**, 1767 (1997); and references therein.
[28] J. Bobroff *et al.*, *Phys. Rev. Lett.* **83**, 4381 (1999).
[29] A. Polkovnikov *et al.*, *Phys. Rev. Lett.* **86,** 296 (2001).
[30] G.-q. Zheng *et al.*, *Physica C* **263**, 367 (1996).
[31] H. Alloul *et al., Phys. Rev. Lett.* **67**, 3140 (1991).
[32] Y. Sidis *et al.*, *Phys. Rev. Lett.* **84**, 5900 (2000).
[33] H. F. Fong *et al.*, *Phys. Rev. Lett.* **82**, 1939 (1999).
[34] K. Tomimoto *et al.*, *Phys. Rev. B* **60**, 114 (1999).
[35] J. Figueras *et al.*, *Supercond. Sci. Technol.* **13**, 1067 (2000).
[36] W. A. MacFarlane *et al.*, *Phys. Rev. Lett.* **85**, 1108 (2000).
[37] K. Ishida *et al.*, *Phys. Rev. Lett.* **76**, 531 (1996).
[38] S. H. Pan, private communications.
[39] G. A. Prinz, *Physics Today* **48**, No.4, 58 (1995).
[40] N.-C. Yeh *et al.*, *Phys. Rev. B* **60**, 10522 (1999).
[41] N.-C. Yeh *et al.*, *Physica B* **284-288**, 507 (2000).
[42] J. Y. T. Wei *et al.*, *J. Appl. Phys.* **85**, 5350 (1999).
[43] K. E. Grey (ed.), *"Nonequilibrium Superconductivity, Phonons and Kapitza Boundaries"*, NATO ASI Series, Plenum, New York (1981).
[44] M. Tinkham, *"Introduction to Superconductivity"*, 2nd ed., McGraw Hill, New York (1996).
[45] R. S. Markiewicz, *J. Phys. Chem. Solids***58**, 1179 (1997).
[46] R. L. Merrill and Q. M. Si, *Phys. Rev. Lett.* **83**, 5326 (1999).
[47] D. L. Novikov *et al.*, *Physica* **210C**, 301 (1993).
[48] T. Siegrist *et al.*, *Nature* **334**, 231 (1988).
[49] M. G. Smith *et al.*, *Nature* **351**, 549 (1991).
[50] J. D. Jorgensen *et al.*, *Phys. Rev. B* **47**, 14654 (1993).
[51] C. U. Jung *et al.*, *cond-mat/0106441*, (2001).
[52] Mun-Seog Kim *et al.*, Preprint.
[53] A. V. Chubukov & N. Gemelke, *Phys. Rev. B* **61**, R6467 (2000).